Science Signaling
AAAS

www.sciencesignaling.org/cgi/content/full/4/189/ra57/DC1

# Supplementary Materials for

## Small Molecule–Mediated Activation of the Integrin CD11b/CD18 Reduces Inflammatory Disease

Dony Maiguel, Mohd Hafeez Faridi, Changli Wei, Yoshihiro Kuwano, Keir M. Balla, Dayami Hernandez, Constantinos J. Barth, Geanncarlo Lugo, Mary Donnelly, Ali Nayer, Luis F. Moita, Stephan Schürer, David Traver, Phillip Ruiz, Roberto I. Vazquez-Padron, Klaus Ley, Jochen Reiser, Vineet Gupta*

*To whom correspondence should be addressed. E-mail: vgupta2@med.miami.edu

Published 6 September 2011, *Sci. Signal.* **4**, ra57 (2011)
DOI: 10.1126/scisignal.2001811

**This PDF file includes:**

**Other Supplementary Material for this manuscript includes the following:**
(available at www.sciencesignaling.org/cgi/content/full/4/189/ra57/DC1)

Movie S1 (.mov format). Neutrophil chemotaxis in 2D in the presence of DMSO (control).
Movie S2 (.mov format). Neutrophil chemotaxis in 2D in the presence of LA1.
Movie S3 (.mov format). Neutrophil chemotaxis in 2D in the presence of LA2.
Movie S4 (.mov format). Neutrophil chemotaxis in 2D in the presence of LA3.
Movie S5 (.mov format). Neutrophil migration in 3D networks in vitro in the presence of DMSO (control).
Movie S6 (.mov format). Neutrophil migration in 3D networks in vitro in the presence of LA1.
Movie S7 (.avi format). Intravital microscopy in TNF-α–treated cremaster muscle with LA1.
Movie S8 (.avi format). Intravital microscopy in TNF-α–treated cremaster muscle with LA1 and the mAb M1/70.

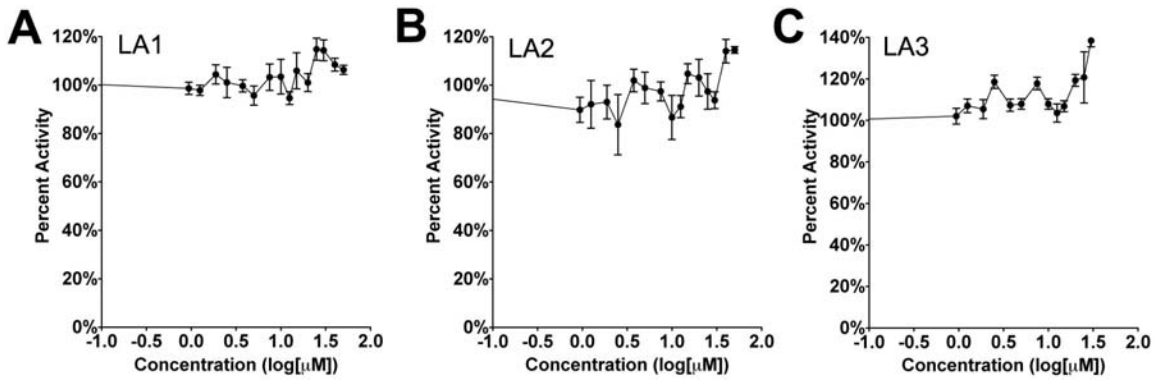


**Fig. S1.** Leukadherins are true agonists and do not inhibit cell adhesion in the presence of the agonist $Mn^{2+}$. Dose-response curves showing the percentage of input K562 CD11b/CD18 cells that adhered to immobilized fibrinogen in the presence of agonist $Mn^{2+}$ ions (1 mM) and in the presence of increasing concentrations of (**A**) LA1, (**B**) LA2, or (**C**) LA3. Data shown are means $\pm$ SEM from three independent wells, and are representative of at least two independent experiments.

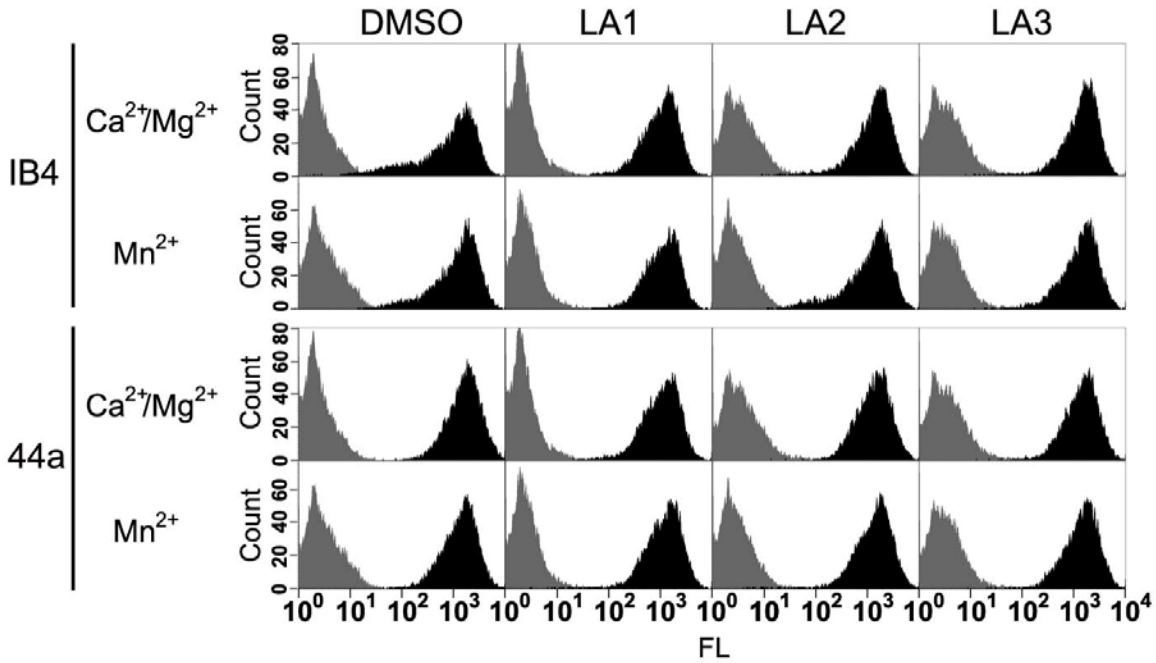


**Fig. S2.** Leukadherins do not affect the surface abundance of CD11b/CD18 on K562 cells. Flow cytometric analysis showing the abundance of CD11b/CD18 on the surface of live K562 CD11b/CD18 cells with the mAbs IB4 and 44a (black) and, as a negative control, isotype IgG2a control mAb (gray). Data shown are representative of at least three independent experiments.

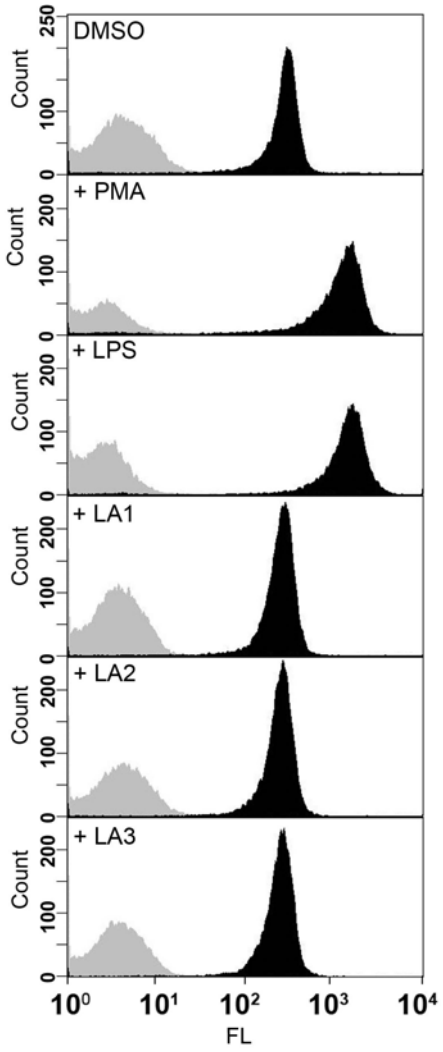


**Fig. S3.** Leukadherins do not mobilize CD11b/CD18 from internal pools or affect the amount of CD11b/CD18 on the surface of human neutrophils. Flow cytometric analysis showing the abundance of CD11b/CD18 on the surface of live human neutrophils with the mAb IB4 (black) and isotype IgG2a mAb as a control (gray). Neutrophils were incubated with antibodies in the presence of vehicle (DMSO), PMA, LPS, or LA1, LA2, or LA3, and were analyzed as described in the Materials and Methods. Data shown are representative of two or three independent experiments.

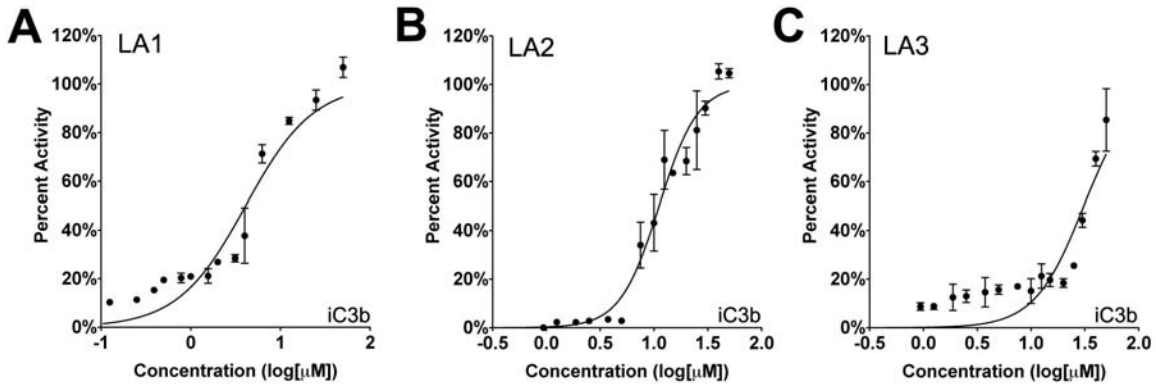


**Fig. S4**. Leukadherins increase the adhesion of CD11b/CD18-expressing cells to iC3b. Leukadherins increased the extent of binding of CD11b/CD18 to iC3b in a dose-dependent fashion. Dose-response curves showing the percentage of input K562 CD11b/CD18 cells that adhered to immobilized iC3b in the presence of increasing amounts of (**A**) LA1, (**B**) LA2, and (**C**) LA3. Data shown are means $\pm$ SEM from six independent wells and are representative of at least three independent experiments.

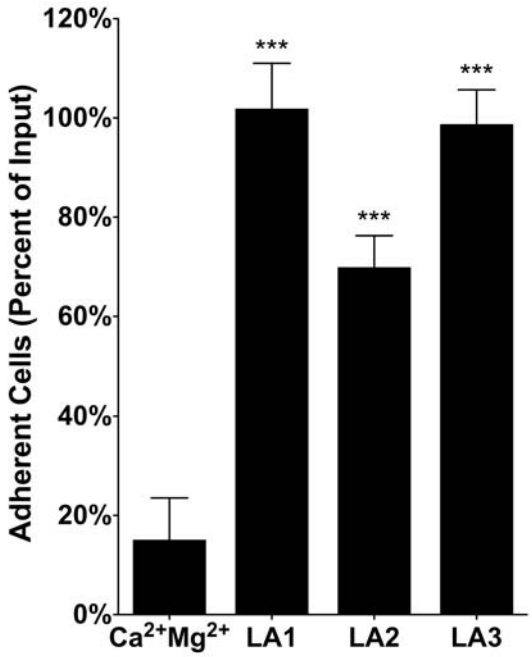


**Fig. S5.** Leukadherin-dependent CD11b/CD18 activation is independent of ligand type. Leukadherins increased the extent of binding of CD11b/CD18 to ICAM-1. Histograms show the relative binding of K562 CD11b/CD18 cells (expressed as a percentage of the number of input cells) that adhered to immobilized ICAM-1 in the presence of buffer alone (containing 1 mM $Ca^{2+}$ and 1 mM $Mg^{2+}$) or LA1, LA2, or LA3. Data shown are means $\pm$ SEM from six to nine independent wells and are representative of at least three independent experiments. ***, $P < 0.0001$.

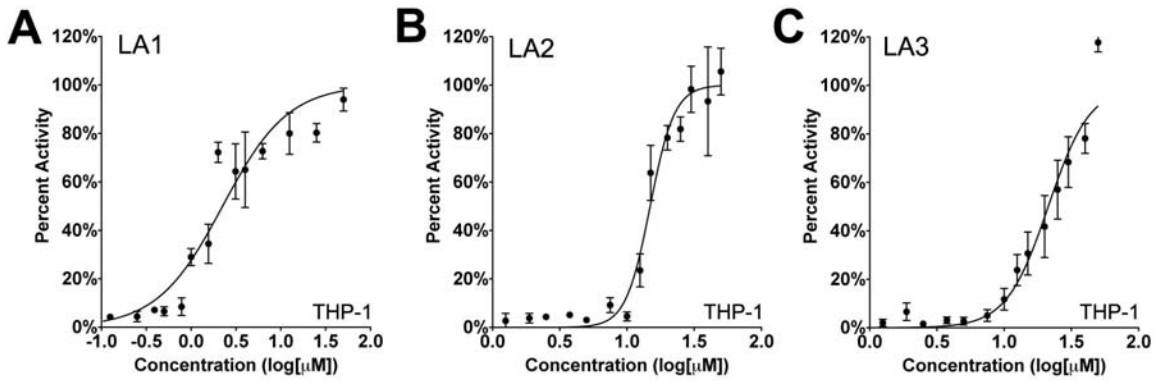


**Fig. S6.** Leukadherin-dependent activation of CD11b/CD18 occurs in THP-1 cells. Leukadherins increase the extent of binding of THP-1 cells to fibrinogen in a dose-dependent fashion. Dose-response curves showing the percentage of input THP-1 cells that adhered to immobilized fibrinogen in the presence of increasing amounts of (**A**) LA1, (**B**) LA2, and(**C**) LA3. Data shown are means $\pm$ SEM from six independent wells and are representative of at least three independent experiments.

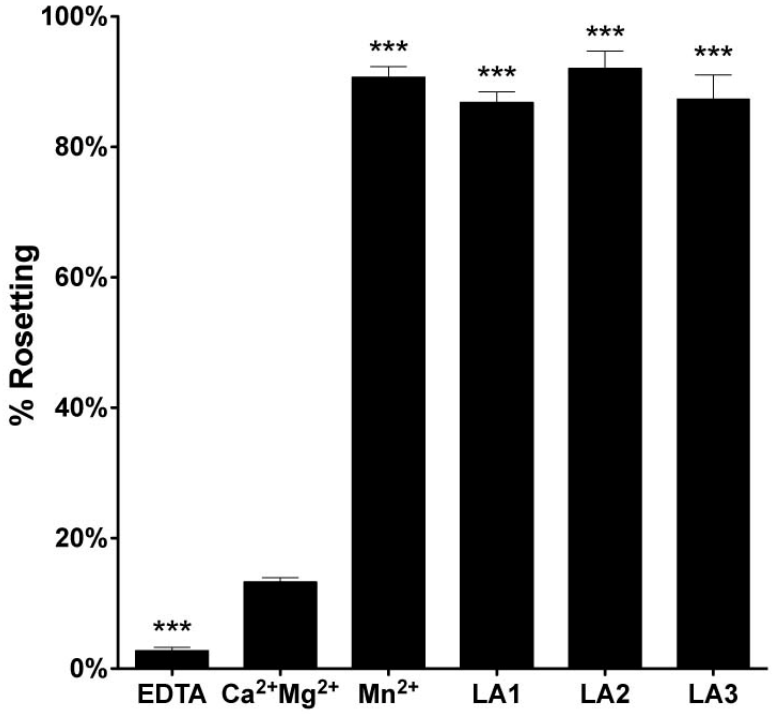


**Fig. S7**. Leukadherins increase the extent of binding of iC3b-coated RBCs by K562 cells. Histograms showing the relative binding of iC3b-opsonized sheep RBCs (EiC3bs) to K562 CD11b/CD18 cells in the presence of EDTA (10 mM), control (1mM $Ca^{2+}$ and 1 mM $Mg^{2+}$), activating $Mn^{2+}$ (1 mM), or LA1, LA2, or LA3 and expressed as the percentage of the total number of cells that formed rosettes. Each histogram represents the mean $\pm$ SEM of triplicate determinations from a representative experiment (one of three performed). ***, $P < 0.0001$.

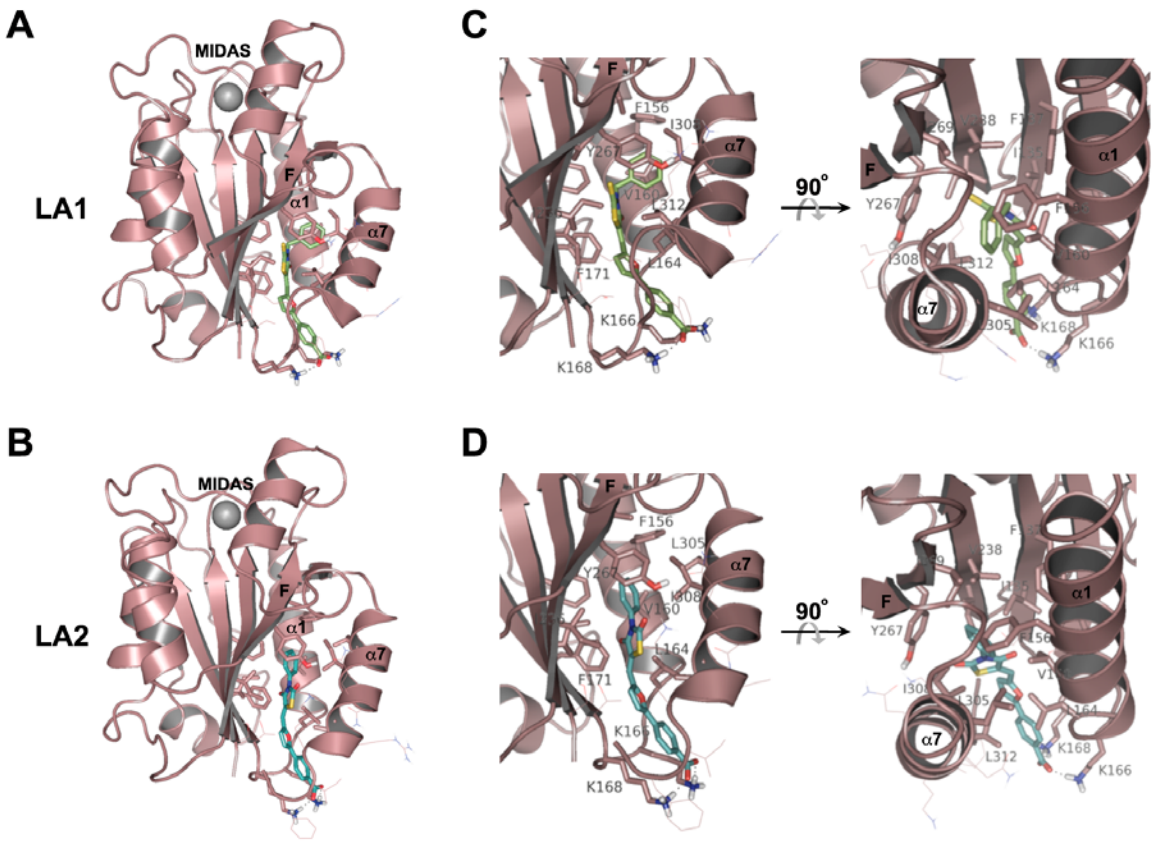


**Fig. S8**. Ribbon diagrams showing computational models for the binding of LA1 and LA2 in an activation-sensitive region of the CD11b A domain. (**A** and **B**) A model of the αA-domain in its open conformation (*1*) (copper ribbon) showing the docking of LA1 (green stick model) and LA2 (blue stick model) in the activation-sensitive F-α7 region. A metal ion at the MIDAS site is shown as a gray sphere. In agreement with our previous computational studies with LA3 (*2*), the leukadherins LA1 and LA2 are positioned such that their most hydrophobic moieties interact with the hydrophobic pocket between helices α7 and α1 and the F-strand. Hydrophobic residues forming the binding pocket (highlighted) include α7 Leu$^{305}$, Ile$^{308}$, and Leu$^{312}$; α1 Phe$^{156}$, Val$^{160}$ and Leu$^{164}$; F-strand Tyr$^{267}$ and Ile$^{269}$; and other hydrophobic pocket residues, including Ile$^{236}$, Val$^{238}$, Ile$^{135}$, Phe$^{137}$, and Phe$^{171}$. The hydophilic carboxylic acid moiety of the leukadherin compounds is positioned away from the hydrophobic pocket, potentially forming ionic interactions with Lys$^{166}$, Lys$^{168}$, or both. (**C**) Magnified views of the activation-sensitive F-α7 region of the αA-domain (copper ribbon) from the docked structure (A). The two views are rotated by 90° with respect to each other. Interacting residues from the activation-sensitive hydrophobic region are shown as copper sticks and are labeled. Dashed lines highlight potential hydrogen bond interactions between LA1 and the αA-domain. (**D**) Magnified views of the activation-sensitive F-α7 region of the αA-domain (copper ribbon) from the docked structure (B). The two views are rotated by 90° with respect to each other. Interacting residues from the activation-sensitive hydrophobic region are shown as copper sticks and are labeled. Dashed lines highlight potential hydrogen bond interactions between LA2 and the αA-domain.

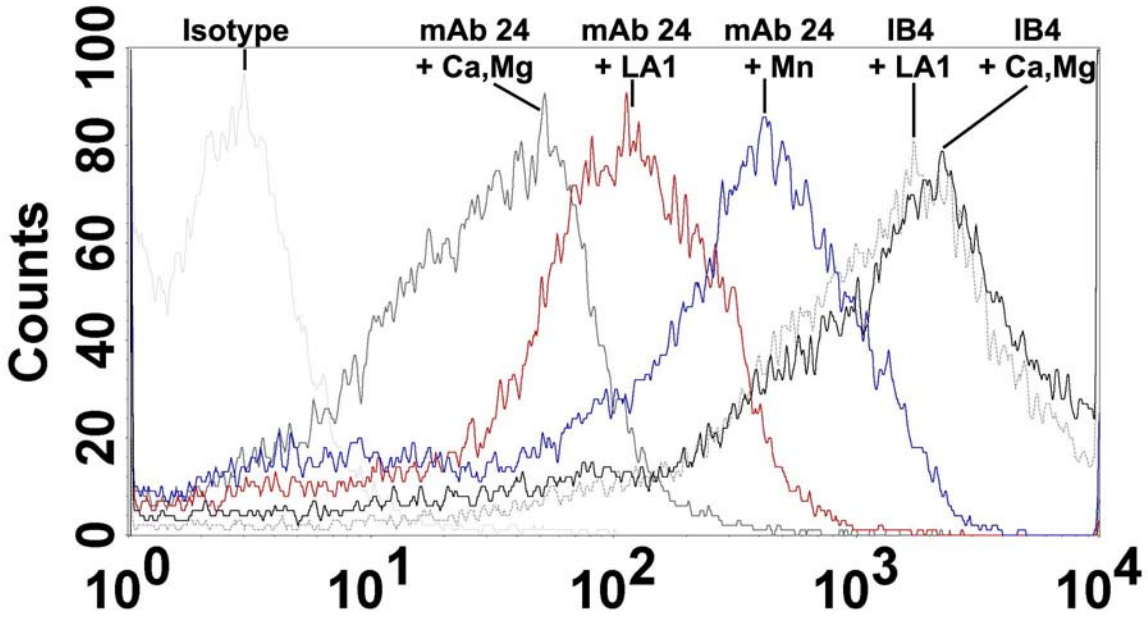


**Fig. S9**. Leukadherins activate full-length CD11b/CD18 on live K562 cells. Flow cytometric analysis showing the reactivity of the activation-sensitive mAb 24 with cell-surface expressed CD11b/CD18 in the absence (+Ca, Mg, dark gray histogram) or presence of LA1 (red histogram) or $Mn^{2+}$ ions (blue histogram). The surface abundance of CD11b/CD18 was analyzed with the mAb IB4 in the absence (+Ca, Mg) or presence of LA1 (black histogram). Binding by the isotype control mAb (light gray) is also shown. Data shown are representative of at least three independent experiments. The data shows an clear increase in mAb24 reactivity with CD11b/CD18 in the presence of LA1 to an extent previously observed with constitutively active CD11b/CD18 (*3*).

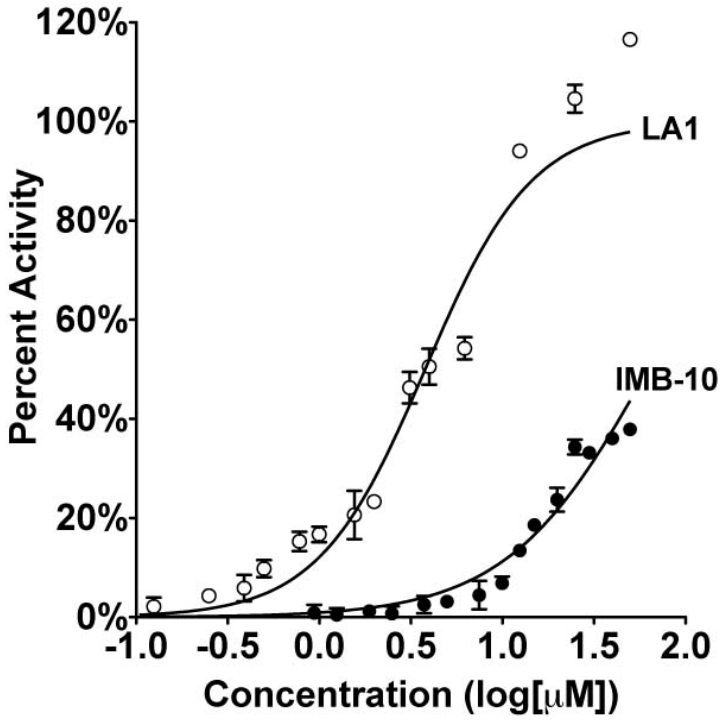


**Fig. S10**. Leukadherins have a higher affinity than does IMB-10 for CD11b/CD18. Dose-response curves show the percentage of input K562 CD11b/CD18 cells that adhered to immobilized fibrinogen in the presence of increasing amounts of LA1 or IMB-10 (*4*) with an $EC_{50}$ value of 4 μM for LA1 and >50 μM for IMB-10. Data shown are means ± SEM from six independent wells and are representative of at least three independent experiments.

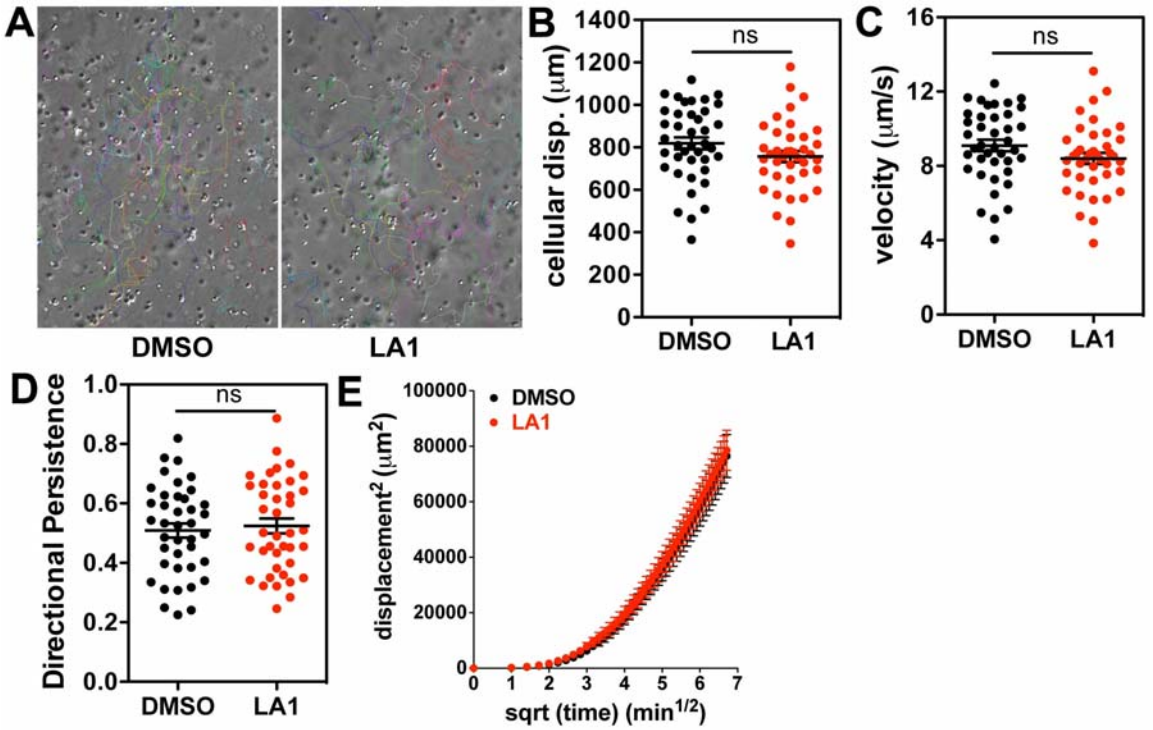


**Fig. S11**. Leukadherins do not affect neutrophil migration in 3D gels in vitro. (**A**) Still images from different time-lapse series imaging WT B6 neutrophils migrating towards a gradient of *f*MLP in 3D collagen gels in the absence (DMSO) or presence of LA1. Migration tracks for 40 individual cells over a period of 45 min from each movie are also presented. (**B** to **E**) Quantitative analyses of at least 40 neutrophils from each condition are also presented and do not show a statistically significant difference in (B) total cellular displacement, (C) migration velocity, or (D) meandering index over the 45-min recording period.(E) A plot of displacement squared versus square root of time shows directed cell-migration under both conditions.

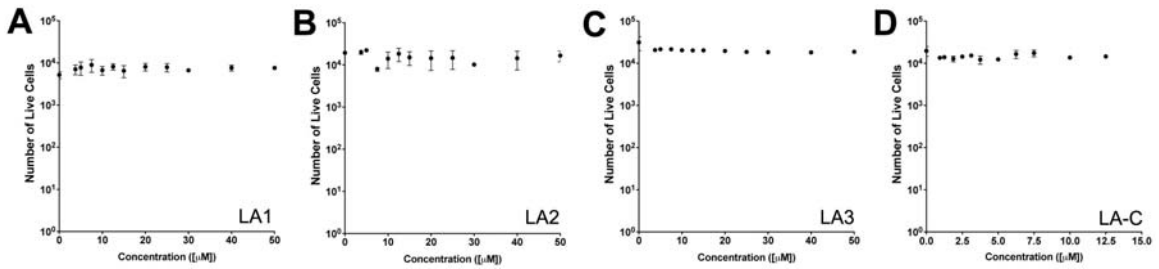


**Fig. S12**. Leukadherins do not cause cytotoxicity in vitro. K562 CD11b/CD18 cells were incubated at 37°C in the presence of increasing amounts of (**A**) LA1, (**B**) LA2, (**C**) LA3, or (**D**) LA-C, and the numbers of live cells were determined after 24 hours. Data shown are means ± SEM from an assay performed in triplicate and are representative of at least two independent experiments. Results show that these compounds are not toxic to cells at concentrations as high as 50 μM.

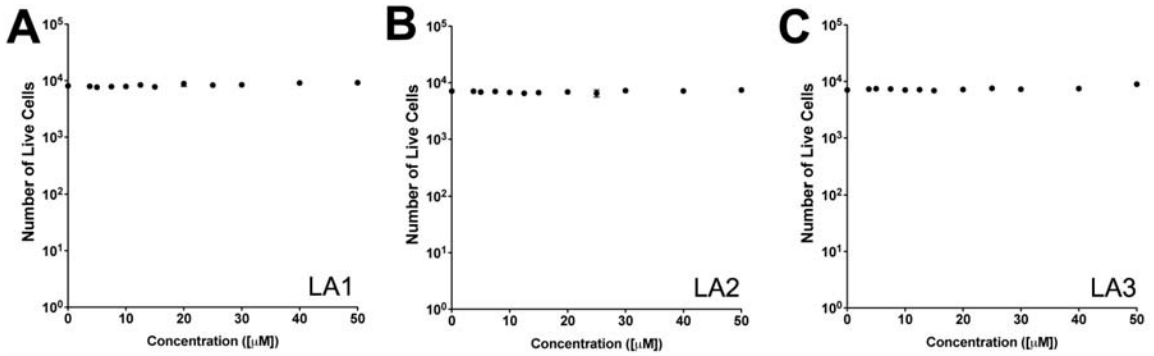


**Fig. S13**. Leukadherins do not cause neutrophil cytotoxicity in vitro. WT B6 neutrophils were incubated at 37°C in the presence of increasing amounts of (**A**) LA1, (**B**) LA2, or (**C**) LA3, and the numbers of live cells were determined with the MTS reagent after a total incubation of 4 hours. Data shown are means $\pm$ SEM from an assay performed in triplicate and are representative of at least two independent experiments. Results show that these compounds were not toxic to primary neutrophils at concentrations as high as 50 μM.

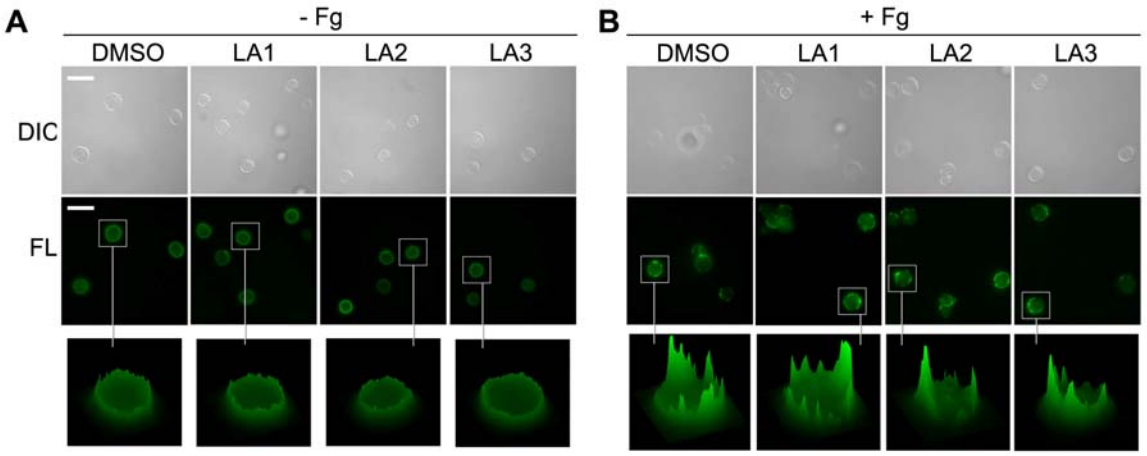


**Fig. S14**. Leukadherins do not induce integrin clustering or outside-in signaling. Fluorescence images of CD11b clustering on the surface of K562 CD11b/CD18 cells surface show that leukadherins do not induce integrin clustering and outside-in signaling. Integrin activation and ligand-binding leads to the clustering of integrins on the cell surface and initiates outside-in signaling (*5*, *6*). Because the compounds LA1, LA2, and LA3 bind to and activate CD11b/CD18, it was possible that such binding alone might trigger integrin-mediated outside-in signaling, thus mimicking a ligand-bound integrin state for the cell, which might have profound consequences on leukocyte lifetime and function. To test this, we used confocal microscopy to imaging CD11b/CD18 clustering on cell surface (*5*). (**A** and **B**) Cell suspensions were incubated with DMSO, LA1, LA2, or LA3 in (A) the absence or (B) the presence of the ligand fibrinogen. Representative fluorescence and DIC images for cells stained for CD11b (green) are shown. Also shown is a 3D representation of CD11b fluorescence intensity for selected cells, analyzed in ImageJ. Scale bar represents 20 μm. Cells displayed no detectable macro clustering of CD11b/CD18 in the absence of ligand (A, DMSO), but showed a high degree of clustering upon addition of exogenous fibrinogen (B, DMSO). Similarly, treatment with LA1, LA2, or LA3 resulted in integrin macro-clustering only upon addition of external fibrinogen, which suggested that LA1, LA2, and LA3 were not integrin ligand mimics.

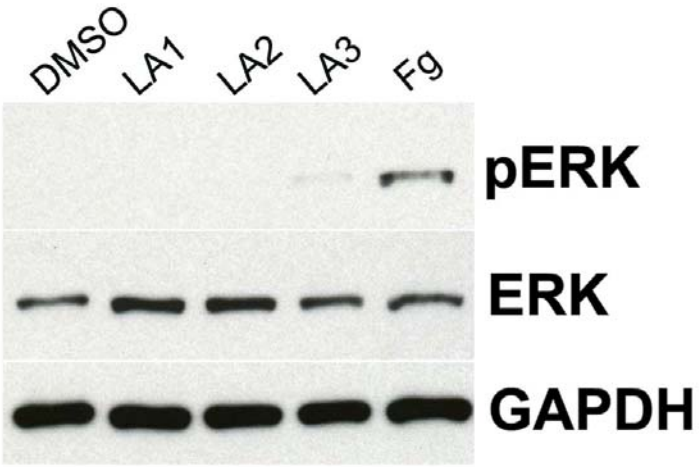


**Fig. S15**. Leukadherins do not induce CD11b/CD18-mediated outside-in signaling. Integrin activation and ligand-binding also initiates outside-in signaling, including the activation of p38 mitogen activated protein kinase (MAPK) and extracellular signal–regulated kinase (ERK) pathways (*5*, *6*), thereby mimicking the anchorage-dependent pro-survival signals in most cells (*7*). Additionally, it synergizes with inflammatory stimuli in potentiating pro-inflammatory nuclear factor κb (NF-κB) signaling (*8*-*10*). Furthermore, although known CD11b/CD18 agonists $Mn^{2+}$ (*11*) and activating mAbs (*12*) and its ligands (*5*) induce ERK1/2 phosphorylation, cells from knock-in animals expressing mutant constitutively active integrins do not (*13*). To examine the effects of LA1, LA2, and LA3, we analyzed the extent of ERK1/2 phosphorylation in treated cells. K562 CD11b/CD18 cells were incubated with DMSO (control), LA1, LA2, LA3, or fibrinogen and the cell lysates were subsequently analyzed by Western blotting with antibodies specific for phosphorylated ERK1/2 (pERK), total ERK1/2, and GAPDH. Whereas LA1, LA2, and LA3 did not induce the phosphorylation of ERK, incubation with fibrinogen or the phorbol ester PMA did (*14*). Data are representative of at least three independent experiments.

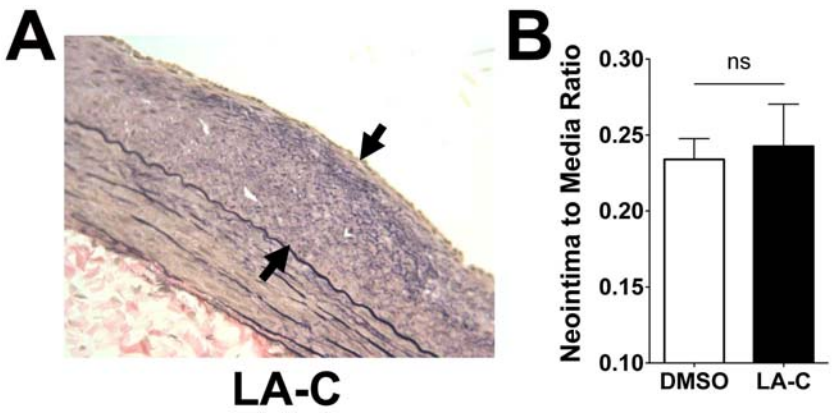


**Fig. S16**. The control compound LA-C has no effect on neointimal thickening upon balloon injury in wild-type rats. (**A**) A representative photomicrograph of rat arteries 21 days after balloon injury from animals treated with the control compound LA-C. Arrows point to the neoinitmal thickening in the artery. (**B**) A bar graph showing the neointima to media ratio determined by morphometric analysis of the injured rat arteries from DMSO- or LA-C-treated animals (n = 7 to 9 animals per treatment). Data shown are means $\pm$ SEM. ns, not significant (by one-way ANOVA).

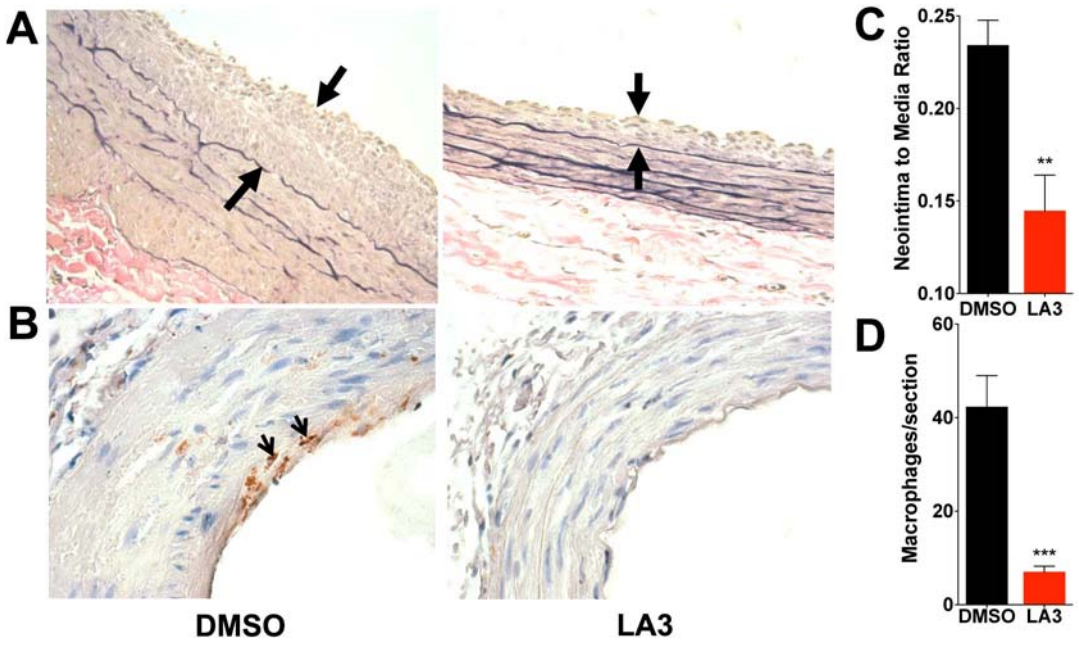


**Fig. S17**. LA3 substantially reduces neointimal thickening after balloon injury in rats. (**A**) Representative photomicrographs of rat arteries 21 days after balloon injury from animals treated with vehicle (DMSO) or LA3. Arrows point to the neoinitmal thickening. (**B**) Photomicrographs of representative arteries 3 days after balloon injury from rats treated with DMSO or LA3. Arrows point to $CD68^{+}$ macrophages. **(C**) A bar graph showing the neointima to media ratio, as determined by morphometric analysis, of the injured arteries from DMSO- or LA3-treated rats (n = 7 to 9 rats per treatment). Data shown are means $\pm$ SEM. **, $P < 0.001$. (**D**) Bar graphs showing quantification of macrophage infiltrates in injured arteries (3 days post injury) from rats treated with DMSO or LA3 (n = 12 rats per group). Data shown are mean $\pm$SEM. ***, $P < 0.0001$.

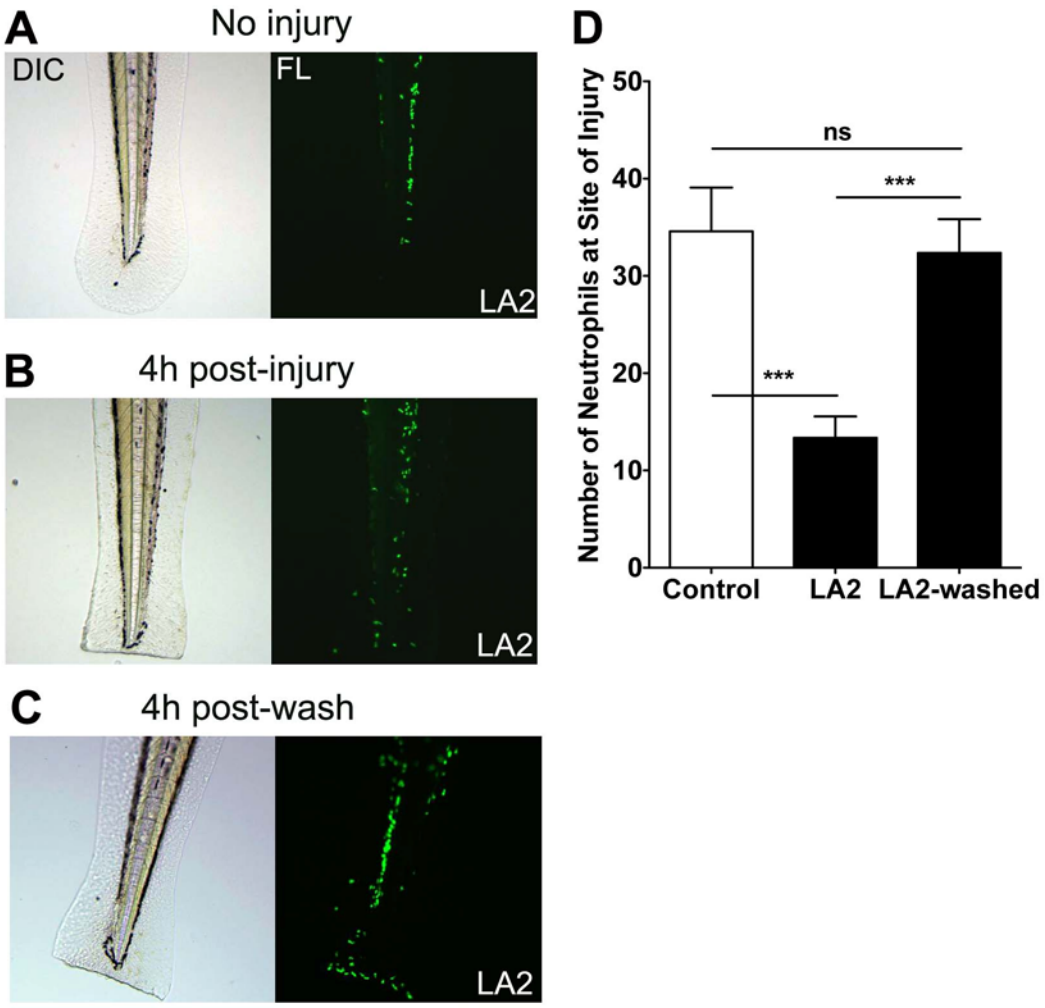


**Fig. S18.** LA2 prevents neutrophil recruitment to injured tissue in a reversible manner. (**A** and **B**) Representative photomicrographs (left) and fluorescence images (right) of the 3dpf larval tail (A) without and (B) with injury from zebrafish treated with LA2 show decreased neutrophil (green) accumulation in the tail, as compared to DMSO-treated zebrafish (Fig. 4, A and B). (**C**) Representative photomicrographs (left) and fluorescence images (right) of the larvae tail showing neutrophil (green) accumulation in the tail 4 hours after the removal of LA2. (**D**) Bar graph showing quantification of the number of neutrophils near the site of tailfin injury in zebrafish larvae treated with vehicle (Control) or LA2, as well as the number of neutrophils near the site of tailfin injury 4 hours after the removal of LA2 (n = 12 to 16 zebrafish larvae per condition). Data shown are means ± SEM. ***, $P < 0.0001$; ns, not significant.

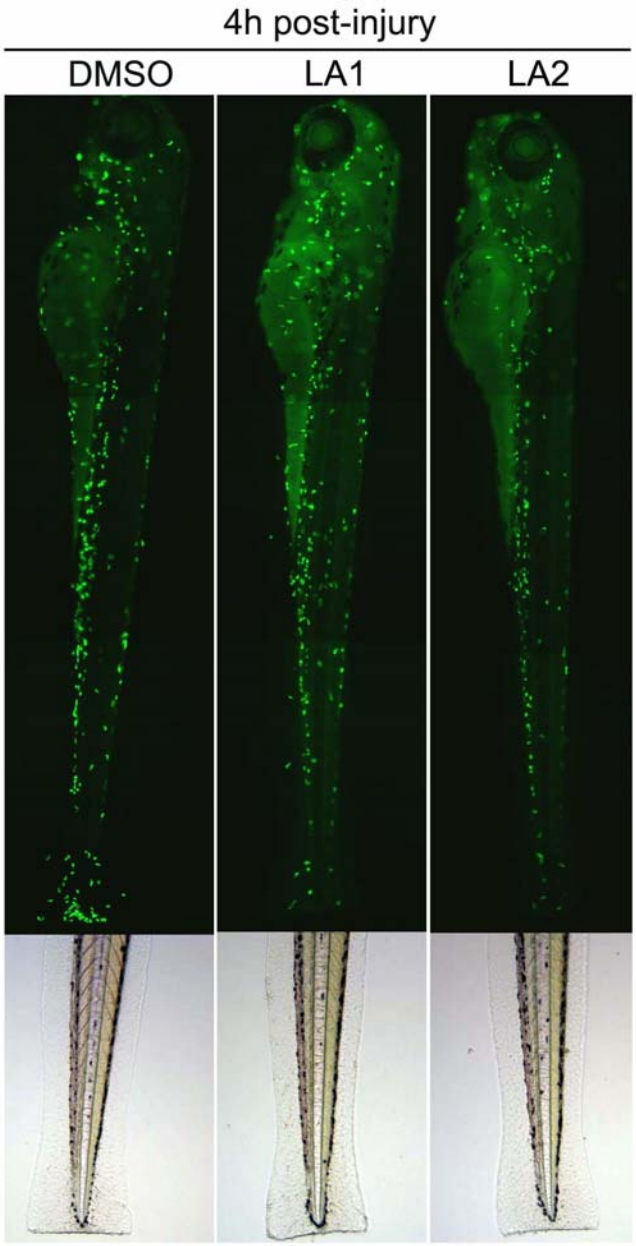


**Fig. S19**. Leukadherins do not lead to loss of neutrophil numbers in zebrafish larvae. Representative fluorescence images of the whole 3dpf zebrafish larvae (top) and photomicrographs of the tails (bottom) from injured fish show neutrophils (green) in each zebrafish larva (n = 12 to 16 zebrafish larvae per group). Zebrafish treated with LA1 or LA2 show slightly higher background green fluorescence because of leukadherin autofluorescence.

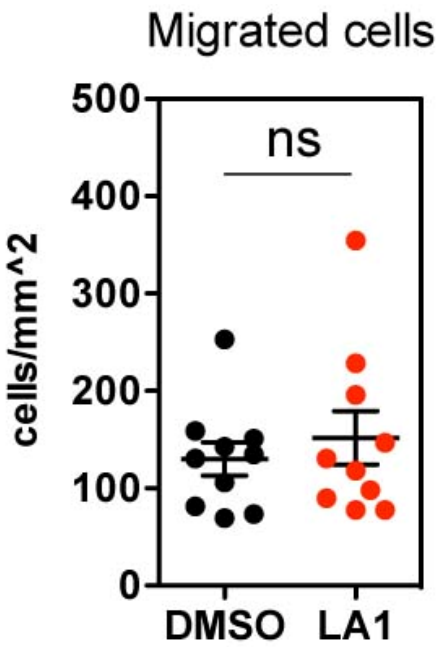


**Fig. S20**. Leukadherins reduce the number of transmigrated cells in vivo. Graph showing intravital microscopy–based quantification of the number of transmigrated neutrophils adjacent to the venules of TNF-α-treated mouse cremaster muscle without (DMSO) or with LA1. Data shown are means ± SEM; ns, no significant difference.

**Table S1.** White blood cell counts in mouse whole-blood samples. Table showing white blood cell counts in whole blood samples from animals treated with saline alone, or with LA1, LA2, or LA3 (n = 3 to 5 animals per treatment); ns, not significant.

| | **Saline** | **LA1** | **LA2** | **LA3** |
|---|---|---|---|---|
| WBC count | $3.6 \pm 1.1 \times 10^3/\mu l$ | $3.4 \pm 0.7 \times 10^3/\mu l$ | $3.8 \pm 1.3 \times 10^3/\mu l$ | $3.8 \pm 0.7 \times 10^3/\mu l$ |
| *P* value | | ns | ns | ns |

**Movie S1**. Neutrophil chemotaxis in 2D in the presence of DMSO (control). A representative WT B6 neutrophil migrating along a gradient of fMLP in the presence of vehicle (DMSO) in a Zigmond chamber. Images were captured at 5-s intervals. The movie represents the movement over 15 min of observation. Bar = 25 μm (.mov, 92kb).

**Movie S2**. Neutrophil chemotaxis in 2D in the presence of LA1. A representative WT B6 neutrophil migrating along a gradient of fMLP in the presence of LA1 in a Zigmond chamber. Images were captured at 5-s intervals. The movie represents the movement over 15 min of observation. Elongated uropods are clearly visible. Bar = 25 μm (.mov, 76kb).

**Movie S3**. Neutrophil chemotaxis in 2D in the presence of LA2. A representative WT B6 neutrophil migrating along a gradient of fMLP in the presence of LA2 in a Zigmond chamber. Images were captured at 5-s intervals. The movie represents the movement over 15 min of observation. Elongated uropods are clearly visible. Bar = 25 μm (.mov, 116kb).

**Movie S4**. Neutrophil chemotaxis in 2D in the presence of LA3. A representative WT B6 neutrophil migrating along a gradient of fMLP in the presence of LA3 in a Zigmond chamber. Images were captured at 5-s intervals. The movie represents the movement over 15 min of observation. Elongated uropods are clearly visible. Bar = 25 μm (.mov, 64kb).

**Movie S5**. Neutrophil migration in 3D networks in vitro in the presence of DMSO (control). A representative movie showing WT B6 neutrophil migrating along a gradient of *f*MLP gradient in 3D collagen gels in the presence of vehicle (DMSO). Images were captured at 60-s intervals. The movie represents the movement over 45 min of observation. Bar = 50 μm (.mov, 3.1Mb). (DIC microscopy, time-lapse 15 frames/s; total number of frames: 45).

**Movie S6**. Neutrophil migration in 3D networks in vitro in the presence of LA1. A representative movie showing WT B6 neutrophil migrating along a gradient of *f*MLP in 3D collagen gels in the presence of LA1. Images were captured at 60-s intervals. The movie represents the movement over 45 min of observation. Bar = 50 μm (.mov, 2.3Mb). (DIC microscopy, time-lapse 15 frames/s; total number of frames: 45).

**Movie S7**. Intravital microscopy in TNF-α-treated cremaster muscle with LA1. A representative movie showing the movement of Lys-EGFP neutrophils in circulation in the presence of LA1 in TNF-α-stimulated cremaster muscle postcapillary venules. Playback speed is 4× (.AVI, 1.4Mb).

**Movie S8**. Intravital microscopy in TNF-α-treated cremaster muscle with LA1 and the mAb M1/70. A representative movie showing the movement of Lys-EGFP neutrophils in circulation in the presence of LA1 and the mAb M1/70 in TNF-α-stimulated cremaster muscle postcapillary venules. Playback speed is 4× (.AVI, 1.4Mb).

**References**


1. J. O. Lee, L. A. Bankston, M. A. Arnaout, R. C. Liddington, Two conformations of the integrin A-domain (I-domain): a pathway for activation? *Structure* **3**, 1333–1340 (1995).
2. M. H. Faridi, D. Maiguel, C. J. Barth, D. Stoub, R. Day, S. Schurer, V. Gupta, Identification of novel agonists of the integrin CD11b/CD18. *Bioorg. Med. Chem. Lett.* **19**, 6902–6906 (2009).
3. V. Gupta, A. Gylling, J. L. Alonso, T. Sugimori, P. Ianakiev, J. P. Xiong, M. A. Arnaout, The beta-tail domain (betaTD) regulates physiologic ligand binding to integrin CD11b/CD18. *Blood* **109**, 3513–3520 (2007).
4. M. Bjorklund, O. Aitio, M. Stefanidakis, J. Suojanen, T. Salo, T. Sorsa, E. Koivunen, Stabilization of the activated alphaMbeta2 integrin by a small molecule inhibits leukocyte migration and recruitment. *Biochemistry* **45**, 2862–2871 (2006).
5. B. B. Whitlock, S. Gardai, V. Fadok, D. Bratton, P. M. Henson, Differential roles for alpha(M)beta(2) integrin clustering or activation in the control of apoptosis via regulation of akt and ERK survival mechanisms. *J. Cell. Biol.* **151**, 1305–1320 (2000).
6. F. G. Giancotti, E. Ruoslahti, Integrin signaling. *Science* **285**, 1028–1032 (1999).
7. E. Pluskota, D. A. Soloviev, D. Szpak, C. Weber, E. F. Plow, Neutrophil apoptosis: selective regulation by different ligands of integrin alphaMbeta2. *J. Immunol.* **181**, 3609–3619 (2008).
8. M. Guha, N. Mackman, The phosphatidylinositol 3-kinase-Akt pathway limits lipopolysaccharide activation of signaling pathways and expression of inflammatory mediators in human monocytic cells. *J. Biol. Chem.* **277**, 32124–32132 (2002).
9. R. Kettritz, M. Choi, S. Rolle, M. Wellner, F. C. Luft, Integrins and cytokines activate nuclear transcription factor-kappaB in human neutrophils. *J. Biol. Chem.* **279**, 2657–2665 (2004).
10. J. P. Luyendyk, G. A. Schabbauer, M. Tencati, T. Holscher, R. Pawlinski, N. Mackman, Genetic analysis of the role of the PI3K-Akt pathway in lipopolysaccharide-induced cytokine and tissue factor gene expression in monocytes/macrophages. *J. Immunol.* **180**, 4218–4226 (2008).
11. K. M. de Bruyn, S. Rangarajan, K. A. Reedquist, C. G. Figdor, J. L. Bos. The small GTPase Rap1 is required for Mn(2+)- and antibody-induced LFA-1- and VLA-4-mediated cell adhesion. *J. Biol. Chem.* **277**, 29468–29476 (2002).
12. C. T Lefort, Y. M. Hyun, J. B. Schultz, F. Y. Law, R. E. Waugh, P. A. Knauf, M. Kim, Outside-in signal transmission by conformational changes in integrin Mac-1. *J. Immunol.* **183**, 6460–6468 (2009).
13. M. Semmrich, A. Smith, C. Feterowski, S. Beer, B. Engelhardt, D. H. Busch, B. Bartsch, M. Laschinger, N. Hogg, K. Pfeffer, B. Holzmann, Importance of integrin LFA-1 deactivation for the generation of immune responses. *J. Exp. Med.* **201**, 1987–1998 (2005).
14. H. Yu, S. J. Suchard, R. Nairn, R. Jove, Dissociation of mitogen-activated protein kinase activation from the oxidative burst in differentiated HL-60 cells and human neutrophils. *J. Biol. Chem.* **270**, 15719–15724 (1995).